

RSC Advances



This article can be cited before page numbers have been issued, to do this please use: D. Mandal, D. Chakraborty, R. V and D. K. Chand, *RSC Adv.*, 2016, DOI: 10.1039/C5RA26721H.



This is an *Accepted Manuscript*, which has been through the Royal Society of Chemistry peer review process and has been accepted for publication.

Accepted Manuscripts are published online shortly after acceptance, before technical editing, formatting and proof reading. Using this free service, authors can make their results available to the community, in citable form, before we publish the edited article. This *Accepted Manuscript* will be replaced by the edited, formatted and paginated article as soon as this is available.

You can find more information about *Accepted Manuscripts* in the [Information for Authors](#).

Please note that technical editing may introduce minor changes to the text and/or graphics, which may alter content. The journal's standard [Terms & Conditions](#) and the [Ethical guidelines](#) still apply. In no event shall the Royal Society of Chemistry be held responsible for any errors or omissions in this *Accepted Manuscript* or any consequences arising from the use of any information it contains.

Group 4 Alkoxide Complexes containing [NNO]-type Scaffold: Synthesis, Structural Characterization and Polymerization Studies

Dipa Mandal, Debashis Chakraborty,* Venkatachalam Ramkumar and Dillip Kumar Chand*

Received 00th January 20xx,
Accepted 00th January 20xx

DOI: 10.1039/x0xx00000x

www.rsc.org/

A series of Ti(IV), Zr(IV) and Hf(IV) complexes are synthesized by complexation of [NNO]-type tridentate Schiff base ligands {2-amino-3-((E)-(2-hydroxybenzylidene)amino)maleonitrile}, **L1(H)**₂; {2-amino-3-((E)-(2-hydroxy-3,5-dimethylbenzylidene)amino)maleonitrile}, **L2(H)**₂ and {2-amino-3-((E)-(3-(*tert*-butyl)-2-hydroxy-5-methylbenzylidene)amino)maleonitrile}, **L3(H)**₂ with suitable group 4 metal alkoxides. The ligands are derived by the mono-condensation of diaminomaleonitrile and salicylaldehyde derivatives. All the complexes are found to be dinuclear on the basis of their NMR and MS spectral data. Three of the nine complexes are structurally characterized by single crystal X-ray diffraction studies. The crystal structures confirmed the dinuclear nature of these complexes. The metal centers of the dinuclear core are connected through two bridging alkoxy groups. The coordination environment of a metal center comprise of one unit of a di-deprotonated ligand, one unit of terminal alkoxide and two units of the bridging alkoxide groups so as to form distorted octahedral complexes. The catalytic activities of these complexes were investigated towards the ring-opening polymerization (ROP) of ϵ -caprolactone (ϵ -CL) and *rac*-lactide (*rac*-LA) under bulk. These complexes were found to be highly active catalysts for the production of PCL [poly(caprolactone)] and PLA [poly(lactic acid)] with high rate of conversion. The strong electron withdrawing cyano groups present in these complexes rationalized the high polymerization activity. The polymers exhibited narrow molecular weight distributions (MWDs). Furthermore, the isolated PLAs were remarkably heterotactic-rich with maximum $P_r=0.80$, by using Hf catalyst with *tert*-butyl substituent on the *ortho*- position of the phenolic moiety. These complexes are moderately active toward the ring-opening homopolymerization of *rac*-epoxides, such as *rac*-cyclohexene oxide (*rac*-CHO), *rac*-propylene oxide (*rac*-PO) and *rac*-styrene oxide (*rac*-SO). These complexes exhibited good activity in ethylene polymerization upon activation with co-catalyst MAO and with a bulky substituent on the *ortho*- position of the phenolic moiety of the catalysts.

Introduction

The development of homogeneous catalysts/initiators for synthesizing ecofriendly biodegradable polymers, such as poly(lactic acid) (PLA), poly(caprolactone) (PCL) and related compounds, from renewable resources is an attractive area of research.¹ In the recent years, such polymers have been extensively utilized as drug delivery excipients, adsorbable sutures, medical implants and scaffolds for tissue engineering.² Catalytic ring-opening polymerization (ROP) of cyclic esters and lactides is considered as the most suitable route to produce these polymers. Various catalytic systems based on the complexes of Al, Zn, Mg, Ca, Sn, Nb, Ta, and selected lanthanides (Nd, Sm, Yb) have been recently employed for the ROP reactions.¹ Several group 4 complexes prepared by using a variety of polydentate chelating ligands have also been employed for ROP, particularly that of lactides (LA) and ϵ

caprolactone (ϵ -CL).³⁻⁵ Reasonably stereoselective PLA have been prepared in the ROP of lactides using some of the above mentioned group 4 complexes.^{3d-f,3j,3o-p,3r-s,3y,4e-f} Group 4 metals are known to exhibit variable coordination number in their complexes. The reactivity of these complexes as catalysts could be tuned by varying the coordination environment around the metal center. The substituents of the ligand framework present in the catalyst play a crucial role in determining the activity and stereoselectivity of ROP using lactide. Kol *et al.*, have reported that the group 4 complexes of dithiodiolate ligands, where the ligand is equipped with electron withdrawing CF₃ groups showed highest catalytic activity for the ROP of *rac*-LA under melt conditions.^{3j} The stereoselectivity of the catalyst is mainly influenced by the central metal and the steric bulk present in the ligand framework. The stereoselectivity in the ROP of *rac*-LA could be increased by increasing the steric bulk at the *ortho*- and *para*-positions of the phenolic ring in group 4 complexes of some bis(phenolate) type ligands.^{3o-p}

Ring-opening homopolymerization of epoxides also have attracted prominent attention for the synthesis of polyethers. Such polyethers are important as they have been frequently

Department of Chemistry, Indian Institute of Technology Madras, Chennai 600 036, Tamil Nadu, India

* Footnotes relating to the title and/or authors should appear here.

Electronic Supplementary Information (ESI) available: [details of any supplementary information available should be included here]. See DOI: 10.1039/x0xx00000x

used as thermoplastic or thermosetting materials, lubricants for textile fibers, adhesive on glass and metals, electrical insulator and foams.⁶ ROP of epoxides such as cyclohexene oxide (CHO), propylene oxide (PO) and styrene oxide (SO) have been accomplished using a variety of Zn, Al, Co, Sc and group 4 metals catalysts.^{5i,j,7} However, the group 4 catalysts were less explored for ROP of the epoxides.^{5i,j,7b-c} Incorporation of electron-withdrawing groups in the ligand moiety of early transition metal complexes have been performed and such complexes exhibited enhanced catalytic activity for the ROP of CHO.^{7c}

Synthetic polymers obtained from olefin polymerization are useful in daily life. High mechanical strength, flexibility, superior toughness, chemical inertness and high tensile strength are the reasons for various applications of synthetic polymers. A large number of catalysts based on transition and inner transition metals have been developed for olefin polymerization, especially that of ethylene.⁸⁻⁹ Fujita *et al.*, reported the use of group 4 complexes of phenoxy-imines as catalysts for ethylene polymerization.^{8a,10} Subsequently, excellent catalysts for ethylene polymerization were developed using fluorinated phenoxyimines^{9a,9d} and bulky substituent bearing phenoxyimines^{8a,9b,9g} as catalysts. Group 4 complexes bearing coordinated alkoxide moieties, in addition to the main ligand frame, have also been developed as active catalysts for olefin polymerization, in presence of the co-catalyst MAO.^{5g-k,9e,9j}

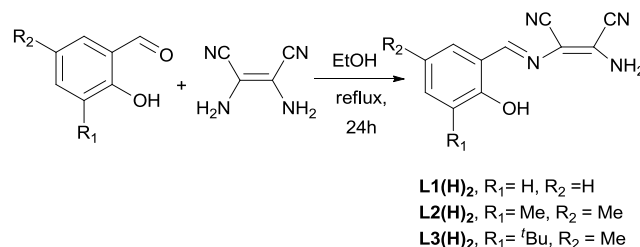
In this work, a series of new group 4 metal complexes of a variety of salicylaldiminato ligands are prepared and used as catalysts/initiators for the preparation of polymers. The Schiff base ligands prepared by the mono-condensation of diaminomaleonitrile with salicylaldehyde derivatives are used for complexation with group 4 metal alkoxides. Each of the ligands is crafted with electron withdrawing cyano group whereas the steric bulk is varied on the ligands by varying the substitution in the salicylaldehyde moiety. The complexes formed are invariably dinuclear in nature where each metal center contains one terminal and two bridging alkoxide groups. The metal complexes are used as catalysts/initiators for ROP of *rac*-LA, ϵ -CL, and *rac*-epoxides. The coordinated alkoxide groups present in the catalysts helped to initiate the polymerization reactions. The complexes are also used as pre-catalysts for ethylene polymerization. The cyano group and steric bulk introduced in the ligand moieties proved beneficial and assisted to elevate the catalytic efficiency of the complexes.

Results and discussion

Synthesis of the ligands, **L1(H)₂**-**L3(H)₂**

The ligand **L1(H)₂** is reported whereas **L2(H)₂** and **L3(H)₂** are new compounds.¹¹ All the ligands were synthesized following the reported procedure of the synthesis of **L1(H)₂** (see Scheme 1) by mono-condensation of diaminomaleonitrile (2,3-

diamino-*cis*-2-butenedinitrile) with appropriate salicylaldehyde derivatives in 1:1 ratio. The new ligands were identified by recording their ¹H NMR, ¹³C NMR and EI-MS spectra (Figure S1 to S6 in ESI[†]); the ligands were also characterized by using elemental analysis technique.

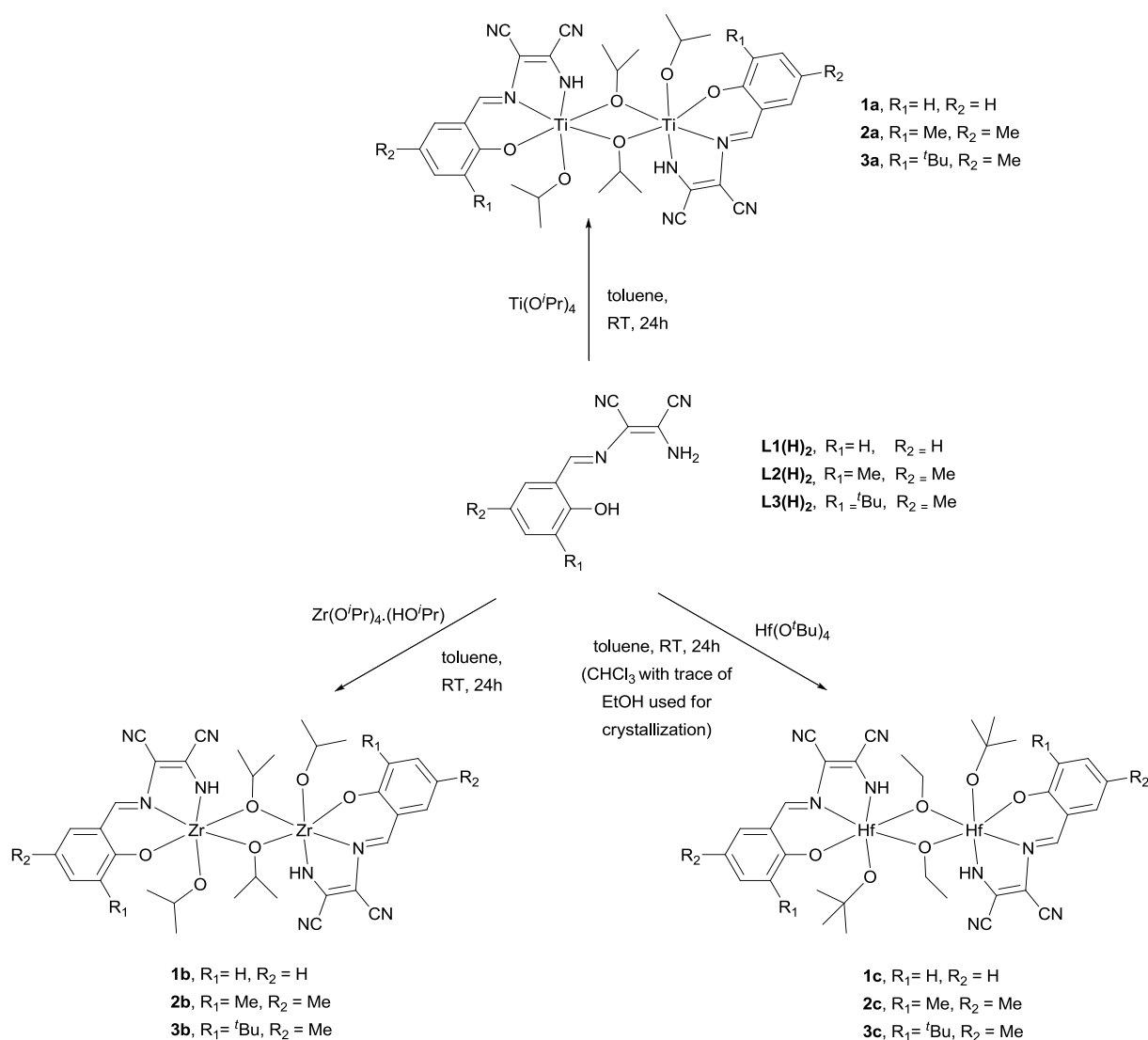


Scheme 1. Synthesis of the ligands **L1(H)₂**-**L3(H)₂**

Synthesis of the group 4 complexes, **1a-3a**, **1b-3b** and **1c-3c**.

The synthetic route for the preparation of all the complexes is shown in the Scheme 2. The complexes were prepared by reacting the ligands **L1(H)₂**-**L3(H)₂** respectively with Ti(O^{*i*}Pr)₄, Zr(O^{*i*}Pr)₄(HO^{*i*}Pr) and Hf(O^{*t*}Bu)₄ in a 1:1 molar ratio in dry toluene at room temperature. After completion of the reactions, toluene was evaporated to dryness. The crude products so obtained were recrystallized from dichloromethane or chloroform for further characterization. All the complexes were identified by recording their ¹H NMR, ¹³C NMR and EI-MS spectra (Figure S7 to S33 in ESI[†]); the complexes were also characterized by using elemental analysis technique. EI-MS characterization reveals that these compounds exist in the dimeric state.

The appearances and pattern of the ¹H NMR spectra of all the Ti and Zr complexes are comparable with each other. However, the extent of shift of the peaks as compared to the corresponding ligands differs on a case to case basis. The ¹H NMR spectrum of a typical complex exhibited one singlet corresponding to the secondary aldimine protons; however, two sets of signals corresponding to two types of isopropoxide groups at 1:1 ratio were observed. The peak corresponding to the phenolic hydrogen disappeared, which indicated phenolate formation. Mono-deprotonation of the amine group occurred during the complex formation as confirmed from the appreciable downfield shift of the signal where the integration ratio decreased to half of the original value (amido formation). The integration ratio of the peaks confirmed only two units of isopropoxide for each unit of the ligand. All these observation supported the di-deprotonation of the ligand unit due to loss of phenolic proton and one of the two amine protons. On the basis of the NMR study presented in this work and related literature, we assumed formation of binuclear complexes that possess equal number of terminal and bridging isopropoxide groups.^{3f,3y,5e,5k} The EI-MS data (see Experimental Section and in ESI[†]) indicated molecular formula corresponding to [M(L)(O^{*i*}Pr)₂]₂ for all the Ti and Zr complexes where L stands for the di-deprotonated ligand.



Scheme 2. Synthesis of the group 4 complexes, **1a-3a**, **1b-3b** and **1c-3c**.

The ^1H NMR data of one of the Ti complexes (**3a**) is described here. The ^1H NMR spectrum of **3a** in CDCl_3 at room temperature displayed signals assignable to two types of isopropoxide groups, *i.e.* terminal and bridging isopropoxide groups. The terminal isopropoxide groups exhibited one well-resolved doublet at $\delta = 1.00\text{--}1.01$ ppm [$\text{O-CH}(\text{CH}_3)_2$] and a multiplet at $4.14\text{--}4.16$ ppm [$\text{O-CH}(\text{CH}_3)_2$]. The bridging isopropoxide groups exhibited one doublet at $1.20\text{--}1.21$ ppm [$\text{O-CH}(\text{CH}_3)_2$] and a multiplet at $4.58\text{--}4.63$ ppm [$\text{O-CH}(\text{CH}_3)_2$]. The two aromatic protons located at 7.15 and 7.37 ppm, and the secondary aldimine proton [$\text{CH}=\text{N}$] at 8.63 ppm are slightly downfield shifted as compared to the signal for the corresponding protons in the free ligand (Figure S34 in the ESI †).

The signal due to the coordinated amide group appeared at 6.26 ppm that is downfield shifted by 1.25 ppm as compared to the free ligand. The ^1H NMR spectra of **3a** in CDCl_3 at variable temperature displayed no change in the signals patterns as obtained at room temperature (Figure S35 in the ESI †). The NMR spectra of **3a** in deuterated toluene displayed only the solvent peaks, due to lack of solubility.

The ^1H and ^{13}C NMR spectra of all the Ti and Zr complexes are provided in ESI † . The NMR spectra support dimeric complex formation as understood from the literature.^{3f,3y,5e,5k} Therefore, the molecular formula of all the Ti and Zr complexes could be generalized as $[\text{M}(\text{L})(\text{O}^i\text{Pr})(\mu\text{-O}^i\text{Pr})_2]$.

The ^1H NMR spectra of all the Hf complexes are comparable with each other. The counter anion of the Hf salt that was used for complexation is *tert*-butoxide where as in the case of Ti and Zr it is isopropoxide. The ^1H NMR of a typical Hf complex exhibited one singlet corresponding to the secondary aldimine protons. As per the data of Ti and Zr complexes, one may presume two types of *tert*-butoxide groups in the Hf complex. However, only one type of *tert*-butoxide group was observed and the number of such group is one per ligand unit. Interestingly, one more set of signals assignable to ethoxide group was observed, that too one per ligand unit. It is proposed, on the basis of literature, that the ethoxide group was derived from the ethanol present in solvent of crystallization *i.e.* chloroform.⁵¹ The integration ratio of the peaks confirmed only one unit of *tert*-butoxide and one unit of ethoxide for each unit of the ligands. Here also the di-deprotonated ligands are present in the complexes. The EI-MS data indicated molecular formula corresponding to $[\text{M}(\text{L})(\text{O}^t\text{Bu})(\text{OEt})_2]_2$ for all the Hf complexes where L stands for the di-deprotonated ligand. Assigning ethoxide for the terminal or bridging position, so also for *tert*-butoxide is not possible from the ^1H NMR spectrum. However, the bulky *tert*-butoxide and relatively smaller ethoxide groups are proposed to occupy terminal and bridging positions, respectively, on the basis of steric consideration. It was confirmed by crystal structure of one of the complexes *i.e.* **3c**. The ^1H and ^{13}C NMR spectra of all Hf complexes are provided in the ESI. Therefore, the molecular formula of all the Hf complexes could be generalized as $[\text{M}(\text{L})(\text{O}^t\text{Bu})(\mu\text{-OEt})_2]_2$.

X-ray diffraction studies of complexes of $[\text{Ti}(\text{L3})(\text{O}^i\text{Pr})_2]_2$, **3a**; $[\text{Zr}(\text{L3})(\text{O}^i\text{Pr})_2]_2$, **3b** and $[\text{Hf}(\text{L3})(\text{O}^t\text{Bu})(\mu\text{-OEt})_2]_2$, **3c**.

The solid state structures of the binuclear complexes **3a**, **3b** and **3c** were determined by single crystal X-ray crystallography analysis and presented in Figures 1-3, respectively. The crystallographic parameters are collected in the Table S1 in ESI†. The complexes **3a**, **3b** and **3c** crystallized in monoclinic (space group *C2/c*), triclinic (space group *P1*), and triclinic (space group *P1*) systems, respectively. With regard to the structural configuration, the molecular structures of all the complexes are rather similar to one another. In a given complex both the metal centers are hexa-coordinated with distorted octahedral geometry. The coordination environment of a metal center is defined by one [ONN]-type tridentate di-deprotonated ligand, one terminal alkoxide group and two bridged alkoxide groups. The ligand units are disposed in a *meridional* fashion and the bridged alkoxides are located *cis* to each other. The terminal alkoxides that are located in different metal centers are disposed in an *anti*-fashion with respect to each other. The relative positions of the ligand units should also be described here to provide a complete picture of the overall coordination environment. This could be defined in more than one way to offer the same meaning, e.g. by mentioning the relative positions of the phenolate oxygen atoms coordinated to different metal centers of the complex.

The phenolate oxygen atoms are actually positioned *anti* to each other in their crystal structures. The geometry of N-H hydrogen atoms in all complexes is “endo”. The bond distances for M–O_{terminal alkoxide} bonds, M–O_{phenoxide} bonds, and M–N_{imine} bonds are comparable to the literature.^{3f} The bond distances for the M–O_{bridging alkoxide} for Ti and Zr complexes where the alkoxide stands for isopropoxide are comparable with literature data.^{3c,3f,3h,5e,5k}

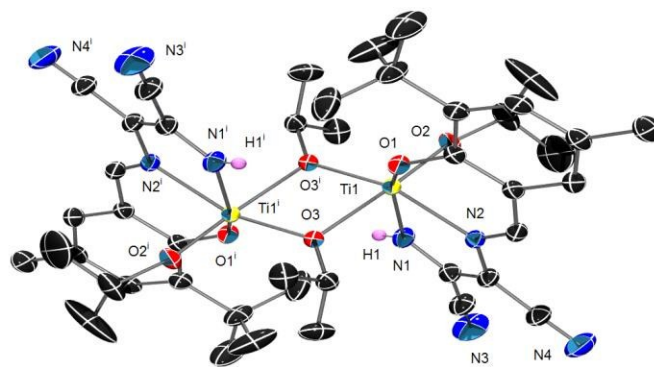


Figure 1. Molecular structure of **3a** with thermal ellipsoids drawn at the 30% probability level. All hydrogen atoms except the amido protons have been omitted for clarity. Selected Bond Distances (Å) and Angles (°): Ti(1)–O(1) 1.8972(13), Ti(1)–O(2) 1.7466(14), Ti(1)–O(3) 2.1538(13), Ti(1)–N(1) 2.0912(16), Ti(1)–N(2) 2.2047(15), Ti(1)–Ti(1') 3.2343(6); O(2)–Ti(1)–O(3) 176.59(6), O(3)–Ti(1)–N(2) 160.97(6), O(1)–Ti(1)–N(1) 153.70(7).

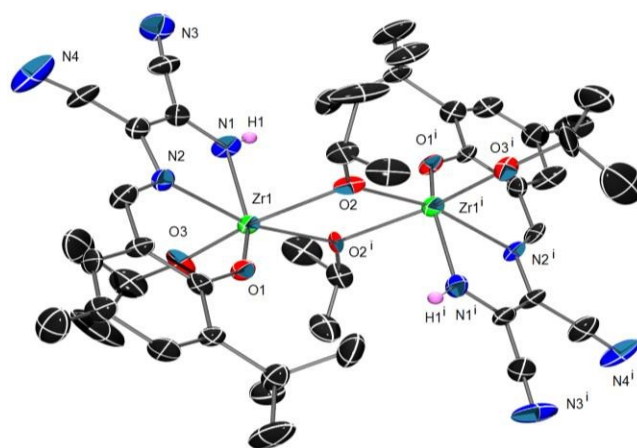


Figure 2. Molecular structure of **3b** with thermal ellipsoids drawn at the 30% probability level. All hydrogen atoms except the amido protons and solvent molecules have been omitted for clarity. Selected Bond Distances (Å) and Angles (°): Zr(1)–O(1) 2.003(3), Zr(1)–O(2) 2.090(3), Zr(1)–O(3) 1.893(3), Zr(1)–N(1) 2.203(4), Zr(1)–N(2) 2.359(3), Zr(1)–Zr(2) 3.5257(9); O(2)–Zr(1)–O(3) 167.75(12), O(1)–Zr(1)–N(1) 144.85(14), O(2)–Zr(1)–N(2) 164.79(12).

However, in the case of Hf the bridging alkoxide is ethoxide and such data is not available in the literature. The distances between two metal atoms in the isopropoxide bridged dinuclear complexes **3a** [3.2343(6) Å] and **3b** [3.5257(9) Å] are closely comparable with the metal-metal distances of some reported complexes of similar designs.^{3f,3y,5e,5k} The dinuclear Hf complex **3c** contains ethoxide bridges and the metal-metal distance in the complex is 3.488(3) Å. There is no ethoxide bridged Hf complex in the literature, hence the present Hf-Hf distance may be considered as a reference for future works.

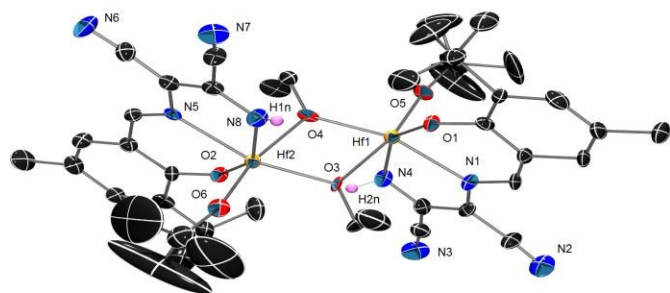


Figure 3. Molecular structure of **3c** with thermal ellipsoids drawn at the 30% probability level. All hydrogen atoms except the amido protons and solvent molecules have been omitted for clarity. Selected Bond Distances (Å) and Angles (°): Hf(1)–O(1) 1.989(12), Hf(1)–O(3) 2.218(10), Hf(1)–O(5) 1.919(11), Hf(1)–N(1) 2.310(14), Hf(1)–N(4) 2.206(14), Hf(1)–Hf(2) 3.4882(3); O(3)–Hf(1)–O(5) 167.6(5), O(4)–Hf(1)–N(1) 160.9(4), O(1)–(Hf1)–N(4) 148.6(5).

The terminal and bridging alkoxide groups in **3a** and **3b** are isopropoxide moieties. The M–O_{alkoxide} bond length related to the bridging alkoxides is relatively longer [Ti–O_{bridging alkoxide} = 2.1538(13) Å, Zr–O_{bridging alkoxide} = 2.090(3) Å] than that of the terminal alkoxides [Ti–O_{terminal alkoxide} = 1.8972(13) Å, Zr–O_{terminal alkoxide} = 1.893(3) Å] for a given metal complex. While the terminal alkoxides are *tert*-butoxide and the bridging alkoxides are ethoxide in **3c**. It is emphasized here that ethoxide bridged dinuclear Hf complexes are not reported in literature. However, there are dinuclear Hf complexes where the bridging units are groups such as oxide, hydroxide, isopropoxide, and phenoxide.^{5e,3i,3h} The Hf–O_{ethoxide} bond length related to the bridging alkoxide is relatively longer [2.222(11) Å] than the Hf–O_{*tert*-butoxide} bond length related to the terminal alkoxide [1.926(11) Å]. Also, the M–N_{imine} bond length [Ti–N_{imine} = 2.2047(15), Zr–N_{imine} = 2.359(3) Å, Hf–N_{imine} = 2.312(14) Å] is also longer than the M–N_{amido} bond length [Ti–N_{amido} = 2.0912(16) Å, Zr–N_{amido} = 2.203(4) Å, Hf–N_{amido} = 2.233(14) Å] for a given metal complex.

ROP of ϵ -CL and *rac*-LA

The performance of all these complexes (**1a-1c**, **2a-2c** and **3a-3c**) towards the ROP of ϵ -CL and *rac*-LA were investigated (Table 1) at 100 and 140 °C respectively. The polymerizations

were performed under solvent free conditions at the monomer to catalyst ratio of 200:1. DOI: 10.1039/C5RA26721H

All the complexes exhibited high catalytic activities towards the ROP of ϵ -CL and *rac*-LA. The PCL and PLA formed exhibit narrow molecular weight distributions [MWDs]. The percentage of monomer (ϵ -CL and *rac*-LA) conversion to product was determined from the integration ratio of relevant protons in the corresponding ¹H NMR spectrum. In case of the ROP of *rac*-LA, the monomer conversions of >97% were obtained within short time of 8, 6, and 5 min using **3a**, **3b** and **3c**, respectively. Thus, the present catalysts could be considered at par with the most active reported group 4 complexes that are used for the ROP reactions.³⁻⁵ The presence of strong electron withdrawing groups, such as cyano, in the ligand backbone increased the Lewis acidity in the metal center and resulted in higher activity. The experimental number-average molecular weight [*M_n*(obs)] and molecular weight distributions (MWDs or PDI) values of polymers were measured by GPC analysis. Among the Ti, Zr and Hf complexes of a given ligand, the polymers obtained by using the Ti complex resulted in the maximum correlation between the *M_n*(theo) and *M_n*(obs). Also, relatively narrow PDI values were observed in case of the polymers obtained by using the Ti complex. An increasing tendency of catalytic activity with an increase of the steric bulk in the form of the *ortho*-substituent on the phenolate ring was observed. The steric bulk increases from **1a** to **2a** to **3a** so also the reactivity. As shown in Table 1, the ROP of *rac*-LA under similar reaction conditions but in presence different Ti complexes *i.e.* **1a**, **2a** and **3a**, required 21, 15 and 8 min, respectively. The reactivity of Zr and Hf complexes also increased with the increase of steric bulk. Such phenomenon of the influence of steric bulk was previously reported for the group 4 complexes of imine-thiobis(phenolate) ligands.^{3p} The introduction of steric bulk at the *ortho*-position of the phenoxide group is likely to protect the metal center of the active catalyst from aggregation and increase the catalytic activity.^{1e} A small discrepancy between the *M_n*(theo) and the *M_n*(obs) were found with slightly broader MWD values. This is attributed to the unavoidable transesterification reactions and/or formation of cyclic oligomers during propagation. Overall the catalytic performance of these complexes is comparable with reported active group 4 catalysts for the ROP of ϵ -CL and *rac*-LA, in terms of *M_n*(obs) and MWD values.³⁻⁵

The microstructure of the PLAs obtained in the ROP of *rac*-LA were investigated by analyzing the homonuclear decoupled ¹H NMR spectra (CDCl₃ at 25 °C) of the PLA samples. The peaks present in the methine region of the spectra were considered for the analysis that indicated the formation of heterotactic-enriched PLAs. The stereochemical structures could be determined from the relative intensity of the tetrads (*isi*, *iii*, *iis/sii*, *sis*) obtained in the homonuclear decoupled ¹H NMR, where “*i*” and “*s*” indicate isotactic and syndiotactic diad, respectively.¹²

Table 1. Results for the ROP of ϵ -CL and *rac*-LA catalyzed by complexes **1a-1c**, **2a-2c** and **3a-3c**^a

Entry	Catalyst	Monomer	Time [min]	Conv. ^b [%]	M_n^c (obs) [kg mol ⁻¹]	M_n^d (theo) [kg mol ⁻¹]	M_w/M_n^c	P_r^e
1	1a	ϵ -CL	10	93	20.45	22.90	1.19	
2	1b	ϵ -CL	7	91	18.36	22.90	1.20	
3	1c	ϵ -CL	6	90	16.65	22.90	1.23	
4	2a	ϵ -CL	9	96	20.98	22.90	1.15	
5	2b	ϵ -CL	6	95	18.05	22.90	1.19	
6	2c	ϵ -CL	5	97	17.89	22.90	1.21	
7	3a	ϵ -CL	4	97	21.18	22.90	1.12	
8	3b	ϵ -CL	4	96	19.45	22.90	1.16	
9	3c	ϵ -CL	3	98	17.34	22.90	1.18	
10	1a	<i>rac</i> -LA	21	92	25.42	28.90	1.17	0.62
11	1b	<i>rac</i> -LA	17	88	21.98	28.90	1.20	0.67
12	1c	<i>rac</i> -LA	15	89	22.33	28.90	1.21	0.70
13	2a	<i>rac</i> -LA	15	96	25.06	28.90	1.15	0.69
14	2b	<i>rac</i> -LA	12	95	24.76	28.90	1.19	0.74
15	2c	<i>rac</i> -LA	10	93	22.90	28.90	1.20	0.75
16	3a	<i>rac</i> -LA	8	98	28.15	28.90	1.14	0.68
17	3b	<i>rac</i> -LA	6	98	25.03	28.90	1.16	0.77
18	3c	<i>rac</i> -LA	5	97	23.43	28.90	1.17	0.80

^aReaction conditions: $[M]_0/[C]_0 = 200:1$, 100 °C for ϵ -CL and 140 °C for *rac*-LA, solvent-free.

^bDetermined from ¹H NMR in CDCl₃ at 25 °C. ^cMeasured by GPC at 27 °C in THF relative to polystyrene standards with Mark-Houwink corrections for M_n . ^d $M_n(\text{theo}) = [M]_0/[C]_0 \times \text{mol wt}(\text{monomer}) + \text{mol wt}(\text{end group})$ at 100% conversion of monomer.

^e P_r is the probability for heterotactic enrichment calculated from homonuclear decoupled ¹H NMR spectrum in CDCl₃ at 25 °C.

In particular, the PLAs obtained from the Hf catalyst (**3c**) with *tert*-butyl groups as substituent on the phenol segment exhibited maximum degree of heterotacticity ($P_r = 0.80$) [Figure S36 in ESI†]. The bulkier substituents led to higher rigidity, especially if they were located at the *ortho*-position of the phenol segment. Previously, Okuda *et al.* have reported the increase of heterotacticity with increasing steric bulk at *ortho*- and *para*-positions of the phenyl ring in (OSSO)-type tetradentate bis(phenolate) ligand for the ROP of *meso*-LA.³⁰ Kol *et al.* have demonstrated the gradual change of tacticity, of the PLA obtained from ROP of *rac*-LA, from heterotactic-rich through atactic to isotactic-rich depending on the substitution pattern of the phenolate ring in the tetradentate-dianionic imine-thiobis(phenolate) type ligand.^{3p} Also, while moving from Ti to Zr to Hf complexes of a given ligand, it was observed that the PLAs produced from Hf and Zr catalysts featured higher degrees of heterotacticity than their Ti counterparts (e.g. $P_r = 0.68$ (**3a**), $P_r = 0.77$ (**3b**), $P_r = 0.80$ (**3c**)).

Furthermore the ROP reactions were done using different monomer-to-catalyst ratios ($[M]_0/[Cat]_0$) in the range of 100:1 to 800:1 using the catalyst **3a** (Figure 4). In the plots of M_n and M_w/M_n (MWD) vs. $[M]_0/[Cat]_0$, the $M_n(\text{obs})$ values of the produced PCLs and PLAs increased proportionally to the monomer-to-catalyst ratios with narrow MWDs, suggesting a good control in the polymerization.

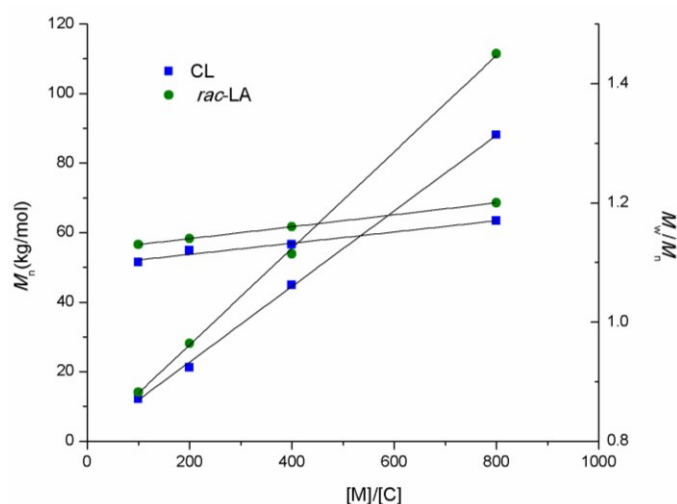


Figure 4. Plots of M_n and M_w/M_n vs. $[M]_0/[Cat]_0$ plots for ROP of ϵ -CL and *rac*-LA at 100 °C and 140 °C respectively using **3a**.

In the plots of M_n and M_w/M_n vs. monomer conversion, the $M_n(\text{obs})$ values increased linearly with the monomer conversion (Figure 5). This linear dependence of $M_n(\text{obs})$ values with the monomer to polymer conversion, supports that the propagating chains grew at nearly constant rate and these polymerizations were well controlled. The plots of % conversion of ϵ -CL and *rac*-LA against time showed a sigmoidal

curve. This curve confirmed that the rate of polymer formation was very high at the initial stage, whereas at a later stage the monomer conversion rate remained constant (Figure S37 in ESI†).

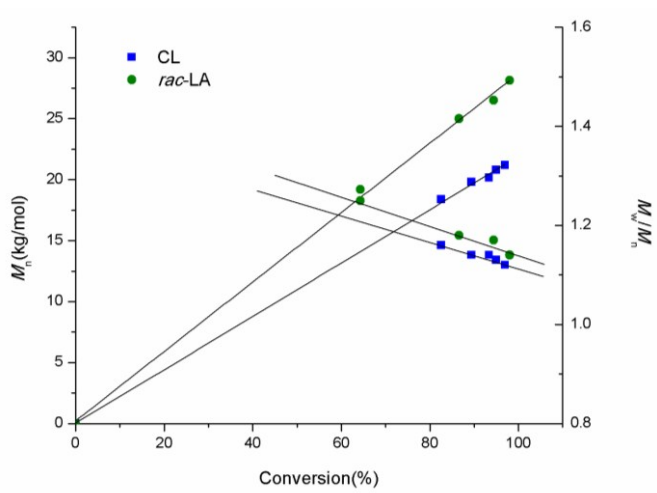


Figure 5. Plots of M_n and M_w/M_n vs. monomer conversion for ROP of ϵ -CL and *rac*-LA at $[M]_0/[Cat]_0=200$ at 100 °C and 140 °C respectively using **3a**.

Mechanistic aspects of the ROP of *rac*-LA.

To find the polymerization mechanism, low molecular weight PLA (oligomer) were synthesized from *rac*-LA at monomer to catalyst ratio 15:1 using catalyst **3a** at 140 °C under solvent-free condition. The end-group analysis of the isolated oligomer was carried out using the techniques like 1H NMR spectroscopy and MALDI-TOF mass spectrometry. The 1H NMR spectrum clearly confirmed the incorporation of an iso-propyl end group ($\delta=1.26$ – 1.28 ppm signals for methyl protons and $\delta=4.16$ – 4.20 signals for methine protons), as shown in Figure S38 in the ESI†.

It suggested that the initiation step occurs with insertion of the coordinated monomer into the M–isopropoxide bond. In addition, the MALDI-TOF mass spectrum of the oligomer incorporates a series of signals with molecular weight interval of 72.04 or 144.10, end-capped with isopropoxide group as acetonitrile adduct, which indicates that isopropoxide moiety acts as the initiating group for the controlled ROP of *rac*-LA (Figure S39 in the ESI†). The expansion of the MALDI-TOF spectrum shows a series of peaks with very small intensity, that corresponds to the intramolecular transesterification and/or cyclic intermediate formation [Figure S40 in ESI†]. The 1H NMR spectrum combined with MALDI-TOF mass spectrum suggested that the ROP proceeds via the coordination-insertion mechanism.^{5g,j}

Kinetic Studies of the ROP of ϵ -CL and *rac*-LA.

View Article Online

DOI: 10.1039/C5RA26721H

Kinetic studies were conducted to find the order of the reaction with respect to monomer and catalyst as well as the rate constant. Polymerizations ϵ -CL and *rac*-LA were monitored over a regular period of time by manual sampling to determine the monomer conversion for $[M]_0/[Cat]_0=200$ at 100 and 140 °C respectively using **3a**.

The ROP mechanism was found to be first order with respect to ϵ -CL and *rac*-LA conversion using **3a**, as clearly elucidated by the linear relationship between semilogarithmic plots ($\ln([M]_{t=0}/[M]_t)$ vs. time (Figure 6). The apparent rate constant (k_{app}) values [$k_{app} = 0.875 \text{ min}^{-1}$ for the ROP of ϵ -CL and $k_{app} = 0.484 \text{ min}^{-1}$ for the ROP of *rac*-LA] were obtained from the slope of these straight lines from the plot of ($\ln([M]_{t=0}/[M]_t)$ vs. time.

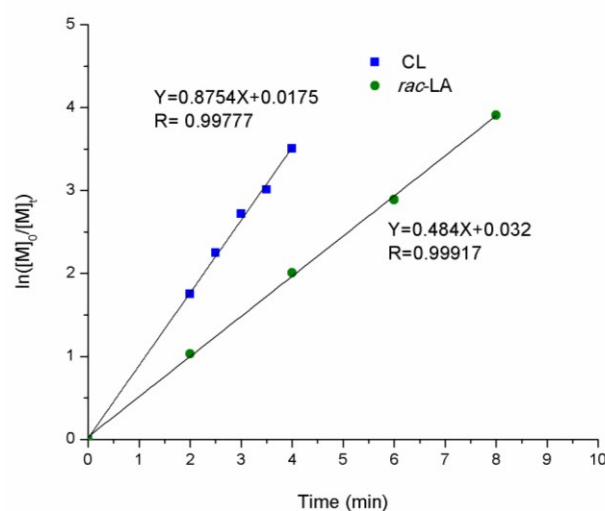


Figure 6. Plots of $\ln([M]_0/[M]_t)$ vs. time (min) for the ROP of ϵ -CL and *rac*-LA at 100 and 140 °C, respectively using **3a** at $[M]_0/[Cat]_0=200:1$.

Ring-Opening homopolymerization of *rac*-CHO, *rac*-PO and *rac*-SO.

Next, the catalytic activities all these complexes (**1a-1c**, **2a-2c** and **3a-3c**) toward the homopolymerization of *rac*-epoxides (*rac*-CHO, *rac*-PO and *rac*-SO) were investigated. All polymerizations were performed under solvent-free conditions in monomer to catalyst ratio 1000:1 under argon atmosphere. The temperature was maintained at 90 °C, 30 °C and 110 °C for CHO, PO and SO respectively as chosen on the basis of literature reports using same epoxide monomer.⁷ The polymerization results are summarized in Table 2.

Table 2. Homopolymerization of *rac*-CHO, *rac*-PO and *rac*-SO catalyzed by **3a-3c**^a

Entry	Catalyst	Epoxide monomer	Time [h]	Conv. ^b [%]	Yield ^c [%]	TOF ^d [h ⁻¹]	M_n^e (obs) [kg mol ⁻¹]	M_w/M_n^e
1	3a	CHO	8	82	80	102.0	31.19	1.29
2	3b	CHO	8	78	75	97.5	29.44	1.33
3	3c	CHO	8	79	77	98.7	28.44	1.34
4	3a	PO	14	68	65	48.5	23.45	1.31
5	3b	PO	14	63	61	45.0	20.05	1.35
6	3c	PO	14	62	59	44.2	21.95	1.37
7	3a	SO	12	72	71	60.0	39.02	1.32
8	3b	SO	12	68	64	56.6	35.56	1.35
9	3c	SO	12	67	65	55.8	36.08	1.36

^aPolymerization conditions: $[M]_0/[C]_0 = 1000$, under solvent-free. Polymerization data using catalysts **1a-1c** and **2a-2c** are given in Table S2 in the ESI. ^bDetermined from ¹H NMR in CDCl₃ at 25 °C. ^cBased on gm of polymer obtained. ^dTurnover frequency (TOF) = Mol of epoxide × (mol of catalyst)⁻¹ h⁻¹. ^eMeasured by GPC at 27 °C in THF relative to polystyrene standards.

Herein all the complexes are moderately active as catalysts for the ROP of epoxides to produce PCHO, PPO and PSO in good yields. The rate of conversion of CHO is comparatively much faster than conversion PO and SO using any of the catalysts (Table 2 and Table S2). For example, in the case of the catalyst **3a**, 82% of CHO conversion (TOF= 102 h⁻¹) was observed after 8 h, whereas only 68% PO conversion (TOF= 48.5 h⁻¹) and 72% SO conversion (TOF= 60.0 h⁻¹) happened even after 14 h and 12 h respectively. All the polymers obtained were characterized by NMR spectroscopy and the experimental number-average molecular weight [M_n (obs)] and molecular weight distributions (MWDs) values of polymers were measured by GPC analysis. All the polymers (PCHO and PSO) were isolated as white solid, except for PPO, which was liquid. The ¹H NMR spectra obtained from the isolated PCHO, PPO and PSO (Figure 7) clearly assigned the characteristic peaks of the respective polymer and signals are comparable with the literature.⁷

For CHO polymerizations, the maximum M_n (obs)= 31.19 was achieved and the MWDs are relatively broader [1.28-1.36]. However, the broader MWDs are comparable with the literature reports for the ROP of CHO using Zn and Al based catalysts.^{7e,7m} This is because of poor initiation and high termination reactions during the polymerization. In case of PO and SO polymerizations, the maximum M_n (obs)= 23.45 and 39.02 were obtained respectively.

Furthermore the plots between yield (%) of polymer vs. time exhibited a sigmoidal curve for the polymerization of CHO, SO and PO using **3a** where $[Epoxide]_0/[Cat]_0 = 1000:1$ (Figure S41 in ESI[†]). This indicates that the yield (%) of polymer increased sharply with the time of polymerization at the initial stages and the yield became constant after a certain time.

Polymerization of Ethylene

The catalysts **1a-1c**, **2a-2c** and **3a-3c** were investigated toward ethylene polymerization (Table 3). However, the catalysts were activated using the co-catalyst MAO (methylaluminoxane). All the polymerization reactions were performed in dry toluene at 60 °C under a constant pressure of ethylene (6 atm, 6.08 bar). The ratio of $[MAO]:[Cat]$ was maintained at 1000:1 in all the reactions.

These complexes are found to be active pre-catalysts towards ethylene polymerization, producing high molecular-weight polyethylene. The high activity of the catalysts is due to the presence of electron withdrawing group (*i.e.* cyano) in the ligand back bone. Presence of electron withdrawing group is known to reduce activation energy of the ethylene insertion reaction and also facilitate the metal-carbon reactivity thereby making the catalyst superior for ethylene polymerization.^{8b} The catalysts **3a-3c** exhibited higher activities, as compared to **2a-2c** and **1a-1c**, and the values fall in the range of 4.81×10^5 to 3.31×10^5 g mol⁻¹ h⁻¹ (Table 3). This is due to the presence of bulky *tert*-butyl groups at the *ortho*- and *para*-positions in the

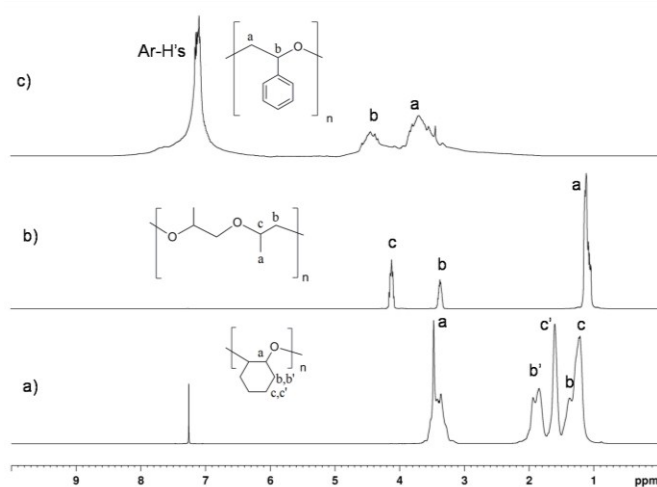


Figure 7. ¹H NMR spectra (500 MHz CDCl₃): a) PCHO; b) PPO; c) PSO.

phenolic moiety of the catalysts **3a-3c**. Some literature reports have shown that presence of steric bulk, on *ortho*-positions in the phenolate ring in the catalysts play a crucial role in improving catalytic activity significantly in ethylene polymerization.^{8a,9b,9g} We have also envisioned that the central metal of the catalyst also has an influence on the catalytic activity. Remarkably, the Ti complexes exhibited maximum activity in contrast to their Zr and Hf analogues under the same catalytic conditions. For ethylene polymerization the tendency of the catalytic activity of the complexes of a given ligand is usually Ti>Zr>Hf.^{9e,f} The higher electrophilicity of the Ti center is the reason behind the higher activity of its complexes in ethylene polymerization.^{8b} Thus, Ti is the most frequently used as metallic center in comparison to Zr and Hf centers for ethylene polymerization.⁸⁻¹⁰

Table 3. Polymerization data for ethylene using complexes **1a-1c**, **2a-2c** and **3a-3c** activated by MAO^a

Entry	Cat.	Yield ^b [gm]	Activity ^c	M_n^d [kg mol ⁻¹]	M_w/M_n^d
1	1a	1.06	2.12	87.89	2.38
2	1b	0.99	1.98	78.92	2.49
3	1c	0.97	1.94	75.45	2.47
4	2a	1.51	3.02	109.11	1.89
5	2b	1.24	2.47	99.35	2.18
6	2c	1.18	2.36	94.26	2.34
7	3a	2.41	4.81	122.75	1.85
8	3b	1.85	3.71	119.50	1.96
9	3c	1.66	3.31	115.29	1.97

^aConditions: 10 μ mol catalyst, [MAO]:[Cat] ratio = 1000, 50 mL toluene, ethylene pressure = 6 atm, at 60 °C for 30 min. ^bgm of polymer obtained after 30 min. ^cActivity in (gm PE/mol cat \times h) $\times 10^5$. ^dMeasured by GPC in 1,2,4-*tri*-chloro benzene (TCB) at 140 °C relative to polystyrene standards.

In order to find the effect of reaction parameters such as, [MAO]/[C] ratio, temperature, and solvent, on the catalytic performance, polymerizations were done systematically by changing such parameters using the catalyst **3a**. To investigate the influence of reaction temperature on the activity, the polymerizations were conducted at different temperatures in the range of 25–80 °C, while the [MAO]/[Cat] molar ratio was kept constant 1000:1. The activity was found to be slightly increased with the elevation of reaction temperature from 25 °C to around 60 °C and then decreased with further increase of temperature [Figure S42 in ESI[†]]. Therefore the reactions were carried out at 60 °C. To find the optimum [MAO]/[Cat] ratio required for maximum catalytic activity, the polymerizations were performed with different [MAO]/[Cat] ratios at 60 °C. The activity increased with increasing of [MAO]/[Cat] ratio and then decreased with further enhancement of [MAO]/[Cat] ratio [Figure S43 in ESI[†]]. The highest activity was obtained at [MAO]/[Cat] ratio = 1000:1. It is proposed that the catalyst is converted into a cationic species when reacted with MAO in line with reported data.¹⁴ The rate of chain propagation in the polymerization increased due to the presence of positive

charge on the metal center. The presence of excess MAO resulted in a reversible deactivation of the active center, therefore resulting in lower activity.^{9k,14} To evaluate the solvent effect on the catalytic performance, the polymerizations have been performed in toluene, dichloromethane and chloroform using [MAO]/[Cat] ratio= 1000:1 at 60 °C. Due to insolubility of these complexes in non polar solvent, the solvents, such as hexane or pentane have not been used in this polymerization. The catalyst **3a** was found to be most active in toluene, whereas in presence of dichloromethane and chloroform a detrimental effect on the catalytic activity was observed [Figure S44 in ESI[†]]. This is in line with the literature.¹⁵⁻¹⁶

Experimental Section

Materials and Methods.

Salicylaldehyde was purchased from Sigma-Aldrich, while 2-hydroxy-3,5-dimethylbenzaldehyde and 3-(*tert*-butyl)-2-hydroxy-5-methylbenzaldehyde were prepared by following literature procedures.¹⁷ Diaminomaleonitrile, group 4 metal salts *i.e.* Ti(O^{*i*}Pr)₄, Zr(O^{*i*}Pr)₄·PrOH and Hf(O^{*t*}Bu)₄; and the co-catalyst MAO were purchased from Sigma-Aldrich and used without further purification. Toluene was dried by refluxing over sodium and benzophenone and distilled under argon prior to use. The deuterated solvent for NMR studies *i.e.* CDCl₃ was acquired from Sigma-Aldrich and purified by distilling over calcium hydride then stored in a glove box. The common reagents and common solvents were acquired locally and purified by usual methods. The monomers namely ϵ -CL, *rac*-CHO, *rac*-PO and *rac*-SO were purchased from Sigma-Aldrich, dried over calcium hydride overnight and distilled freshly prior to use. Lactide monomer, *rac*-LA was purchased from Sigma-Aldrich and purified by sublimation under argon atmosphere and stored in glove box.

All manipulations for the preparation of complexes were carried out using either standard Schlenk techniques or glove box techniques under a dry argon atmosphere. The polymerization reactions were also carried out under argon atmosphere. All ¹H and ¹³C NMR spectra were recorded on a Bruker Avance 400 MHz or 500 MHz spectrometers with chemical shifts given in parts per million (ppm) using residual solvent peak at 7.26 ppm as reference. EI spectra of the compounds were recorded using JEOL GCMATE II instrument. Elemental analyses were performed using a Perkin Elmer Series 11 analyzer. MALDI-TOF MS spectra were recorded on a Bruker Daltonics instrument in dihydroxy benzoic acid matrix. Molecular weights (M_n and M_w) and the MWDs (M_w/M_n) of polymer samples were determined by GPC instrument with Waters 510 pump and Waters 410 or 2414 differential refractometer as the detector. Single crystal XRD data were collected on a Bruker AXS (Kappa Apex 2) CCD diffractometer equipped with graphite monochromated Mo (K α) (λ = 0.7107 Å) radiation source.

Synthesis of the ligands

The new ligands, **L2(H)₂** and **L3(H)₂** were prepared in a similar manner as reported for the known ligand **L1(H)₂**.¹¹

Ligand L1(H)₂: To a solution of 2-hydroxy-benzaldehyde (1 g, 8.19 mmol) in absolute ethanol was added a solution of diaminomaleonitrile (0.874 g, 8.09 mmol) in absolute ethanol. The ligand was formed via monocondensation and the reaction procedure was as per the report.¹¹

Ligand L2(H)₂: To a solution of 2-hydroxy-3,5-dimethylbenzaldehyde (1 g, 6.66 mmol) in absolute ethanol was added solution of diaminomaleonitrile (0.705 g, 6.52 mmol) in absolute ethanol. The mixture was refluxed for 24 h and reddish brown precipitate was observed. The resulting solution was cooled down to room temperature and the a reddish brown precipitate were filtered off, washed with ethanol and dried under vacuum to afford the pure product **L2(H)₂**. Yield 0.81 g, (52%). Mp: 208 °C. ¹H NMR (500 MHz, CDCl₃): δ = 2.24 (s, (CH₃), 3H), 2.28 (s, (CH₃), 3H), 4.95 (s, NH₂, 2H), 7.06 (s, Ar-H, 1H), 7.13 (s, Ar-H, 1H), 8.51 (s, HC=N, 1H), 11.36 (s, Ar-OH, 1H). ¹³C NMR (125 MHz, CDCl₃): δ = 15.4 (Ar-CH₃), 20.4 (Ar-CH₃), 108.0 (CNH₂), 112.0 (NCCNH₂), 113.8 (NCCN), 117.6 (Ar-C), 123.6 (NCCN), 126.0 (Ar-C), 129.2 (Ar-C), 130.9 (Ar-C), 137.3 (Ar-C), 156.5 (Ar-O), 163.0 (HC=N). ESI-MS *m/z* calculated for [M+H]⁺. C₁₃H₁₂N₄O: 241.26 found 241. Anal. Calcd for C₁₃H₁₂N₄O: C 64.99, H 5.03, N 23.32. Found: C 64.97, H 5.01, N 23.31.

Ligand L3(H)₂: The ligand **L3(H)₂** was prepared in a similar manner as described for **L2(H)₂** by using 3-(*tert*-butyl)-2-hydroxy-5-methylbenzaldehyde (1 g, 5.20 mmol) instead of 2-hydroxy-3,5-dimethylbenzaldehyde and diaminomaleonitrile (0.551 g, 5.10 mmol). The resulting yellow precipitate were filtered off, washed with ethanol and dried under vacuum. Yield 0.79 g, (55%). Mp: 185 °C. ¹H NMR (400 MHz, CDCl₃): δ = 1.43 (s, C(CH₃)₃, 9H), 2.33 (s, (CH₃), 3H), 5.01 (s, NH₂, 2H), 7.09–7.10 (d, Ar-H, 1H), 7.27–7.28 (d, Ar-H, 1H), 8.55 (s, HC=N, 1H), 11.79 (s, Ar-OH, 1H). ¹³C NMR (100 MHz, CDCl₃): δ = 20.7 (Ar-CH₃), 29.4 (C(CH₃)₃), 34.9 (C(CH₃)₃), 107.4 (CNH₂), 112.0 (NCCNH₂), 113.5 (NCCN), 118.3 (Ar-C), 122.7 (NCCN), 128.7 (Ar-C), 131.5 (Ar-C), 133.7 (Ar-C), 137.6 (Ar-C), 157.6 (Ar-O), 163.4 (HC=N). ESI-MS *m/z* calculated for [M+H]⁺. C₁₆H₁₈N₄O: 283.34 found 283. Anal. Calcd for C₁₆H₁₈N₄O: C 68.06, H 6.43, N 19.84. Found: C 68.05, H 6.41, N 19.82.

Synthesis of complexes 1a-1c, 2a-2c and 3a-3c

Complex 1a: To a solution of **L1(H)₂** [2-amino-3-((E)-(2-hydroxybenzylidene)amino)maleonitrile] (0.037 g, 0.175 mmol) in 5 mL of dry toluene was added a solution of Ti(O^{*i*}Pr)₄ (0.050 g, 0.175 mmol) in 5 mL toluene, in 1:1 stoichiometric ratio. The reaction mixture was stirred for an additional period of 24 h at room temperature. The resulting brown precipitate was evaporated to dryness under vacuum and crystallized from chloroform solution. Yield 0.06 g, (90%). Mp: 205 °C. ¹H

NMR (500 MHz, CDCl₃): δ = 1.15–1.16 (d, J = 5.5 Hz, CH(CH₃), 6H), 1.18–1.19 (d, J = 5.5 Hz, CH(CH₃), 6H), 4.11–4.17 (m, CH(CH₃)₂, 1H), 4.35–4.41 (m, CH(CH₃)₂, 1H), 6.23 (s, NH, 1H), 6.75–6.78 (d, Ar-H, 1H), 7.00–7.03 (d, Ar-H, 1H), 7.44–7.45 (m, Ar-H, 1H), 7.51–7.53 (m, Ar-H, 1H), 8.37 (s, HC=N, 1H). ¹³C NMR (125 MHz, CDCl₃): δ = 21.5 (CH(CH₃)₂), 24.9 (CH(CH₃)₂), 68.1 (O-CH(CH₃)₂), 71.7 (O-CH(CH₃)₂), 103.2 (CNH), 113.8 (NCCNH), 117.1 (NCCN), 120.7 (Ar-C), 125.4 (Ar-C), 129.1 (NCCN), 133.4 (Ar-C), 136.3 (Ar-C), 138.0 (Ar-C), 153.8 (Ar-O), 158.0 (HC=N). EI-MS *m/z* calculated for [M]⁺. C₃₄H₄₀N₈O₆Ti₂: 752.46 found 752.1491. Anal. Calcd for C₃₄H₄₀N₈O₆Ti₂: C 54.27, H 5.36, N 14.89. Found: C 54.25, H 5.34, N 14.86.

Complex 1b: Ligand **L1(H)₂** (0.027 g, 0.129 mmol) and Zr(O^{*i*}Pr)₄·*i*-PrOH (0.050 g, 0.129 mmol) were reacted in 1:1 stoichiometric ratio and the reaction was carried out in similar manner as described for **1a**. Yield 0.05 g, (88%). Mp: 211 °C (decomp). ¹H NMR (500 MHz, CDCl₃): δ = 1.07–1.09 (d, J = 6 Hz, CH(CH₃)₂, 3H) 1.18–1.19 (d, J = 6 Hz, CH(CH₃)₂, 3H), 1.46–1.47 (d, J = 6 Hz, CH(CH₃)₂, 6H), 4.05–4.07 (m, CH(CH₃)₂, 1H), 4.66–4.68 (m, CH(CH₃)₂, 1H), 6.10 (s, NH, 1H), 6.29–6.31 (d, Ar-H, 1H), 6.56–6.59 (m, Ar-H, 1H), 6.93–6.94 (m, Ar-H, 1H), 7.31–7.34 (m, Ar-H, 1H), 8.36 (s, HC=N, 1H). ¹³C NMR (125 MHz, CDCl₃): δ = 20.7 (CH(CH₃)₂), 21.7 (CH(CH₃)₂), 25.9 (CH(CH₃)₂), 69.6 (O-CH(CH₃)₂), 74.9 (O-CH(CH₃)₂), 104.0 (CNH), 113.1 (NCCNH), 122.3 (Ar-C), 128.3 (NCCN), 128.9 (Ar-C), 129.1 (Ar-C), 133.1 (Ar-C), 135.8 (Ar-C), 136.3 (Ar-C), 155.8 (Ar-O), 158.2 (HC=N). EI-MS *m/z* calculated for [M]⁺. C₃₄H₄₀N₈O₆Zr₂: 839.18 found 839.1240 Anal. Calcd for C₃₄H₄₀N₈O₆Zr₂: C 48.66, H 4.80, N 13.35. Found: C 48.64, H 4.78, N 13.32.

Complex 1c: Ligand **L1(H)₂** (0.022 g, 0.106 mmol) and Hf(O^{*t*}Bu)₄ (0.050 g, 0.106 mmol) were reacted in 1:1 stoichiometric ratio and the reaction was carried out in similar manner as described for **1a**. Yield 0.05 g, (87%). Mp: 217 °C (decomp). ¹H NMR (500 MHz, CDCl₃): δ = 1.07 (s, C(CH₃)₃, 9H), 1.37–1.39 (t, CH₂(CH₃), 3H), 4.28–4.33 (m, CH₂(CH₃), 2H), 6.10 (s, NH, 1H), 7.19–7.20 (m, Ar-H, 2H), 7.36–7.37 (d, Ar-H, 1H), 7.48–7.49 (d, Ar-H, 1H), 8.44 (s, CH=N, 1H). ¹³C NMR (125 MHz, CDCl₃): δ = 21.5 (CH(CH₃)₃), 26.4 (CH₂(CH₃)), 68.0 (O-C(CH₃)₃), 74.0 (O-CH₂(CH₃)), 102.2 (CNH), 113.6 (NCCNH), 121.3 (NCCN), 124.8 (Ar-C), 126.3 (NCCN), 128.3 (Ar-C), 130.0 (Ar-C), 136.1 (Ar-C), 137.8 (Ar-C), 155.8 (Ar-O), 158.8 (HC=N). EI-MS *m/z* calculated for [M]⁺. C₃₄H₄₀N₈O₆Hf₂: 1013.71 found 1013.8488 Anal. Calcd for C₃₄H₄₀N₈O₆Hf₂: C 40.28, H 3.98, N 11.05. Found: C 40.26, H 3.96, N 11.02.

Complex 2a: Ligand **L2(H)₂** [2-amino-3-((E)-(2-hydroxy-3,5-dimethylbenzylidene)amino)maleonitrile] (0.042 g, 0.175 mmol) and Ti(O^{*i*}Pr)₄ (0.050 g, 0.175 mmol) were reacted in 1:1 stoichiometric ratio and the reaction was carried out in similar manner as described for **1a**. Yield 0.07 g, (92%). Mp: 186 °C. ¹H NMR (500 MHz, CDCl₃): δ = 1.07–1.08 (d, J = 6.5 Hz, CH(CH₃)₂, 6H), 1.30–1.32 (d, J = 6.5 Hz, CH(CH₃)₂, 6H), 2.44 (s, (CH₃), 3H), 2.49 (s, (CH₃), 3H), 4.22–4.25 (m, CH(CH₃)₂, 1H), 4.54–4.57 (m, CH(CH₃)₂, 1H), 6.68 (s, NH, 1 H), 7.36 (s, Ar-H, 1H), 7.46 (s, Ar-H, 1H), 8.46 (s, HC=N, 1H). ¹³C NMR (125 MHz, CDCl₃): δ = 18.2

(CH(CH₃)₂), 20.4 (CH(CH₃)₂), 25.7 (Ar-CH₃), 31.0 (Ar-CH₃), 68.1 (O-CH(CH₃)₂), 73.7 (O-CH(CH₃)₃), 103.0 (CNH), 113.9 (NCCNH), 120.9 (NCCN), 125.4 (Ar-C), 129.7 (NCCN), 131.3 (Ar-C), 136.0 (Ar-C), 138.0 (Ar-C), 138.4 (Ar-C), 154.3 (Ar-O), 160.7 (HC=N). EI-MS *m/z* calculated for [M+H]⁺. C₃₈H₄₈N₈O₆Ti₂: 809.57 found 809.6174. Anal. Calcd for C₃₈H₄₈N₈O₆Ti₂: C 56.45, H 5.98, N 13.86. Found: C 56.43, H 5.96, N 13.84.

Complex 2b: Ligand **L2(H)₂** (0.031 g, 0.129 mmol) and Zr(O^{*i*}Pr)₄·PrOH (0.050 g, 0.129 mmol) were reacted in 1:1 stoichiometric ratio and the reaction was carried out in similar manner as described for **1a**. Yield 0.05 g, (90%). Mp: 202 °C (decomp). ¹H NMR (500 MHz, CDCl₃): δ = 1.07–1.09 (d, J = 6 Hz, CH(CH₃)₂, 3H), 1.20–1.21 (d, J = 6 Hz, CH(CH₃)₂, 3H), 1.44–1.45 (d, J = 6.5 Hz, CH(CH₃)₂, 6H), 2.48 (s, (CH₃), 3 H), 2.53 (s, (CH₃), 3H), 3.96–3.98 (m, CH(CH₃)₂, 1H), 4.37–4.45 (m, CH(CH₃)₂, 1H), 6.21 (s, NH, 1H), 7.32 (s, Ar-H, 1H), 7.55 (s, Ar-H, 1H), 8.55 (s, HC=N, 1H). ¹³C NMR (125 MHz, CDCl₃): δ = 20.4 (Ar-CH₃), 24.9 (Ar-CH₃), 25.5 (CH(CH₃)₂), 25.6 (CH(CH₃)₂), 30.4 (CH(CH₃)₂), 72.9 (O-CH(CH₃)₂), 75.0 (O-CH(CH₃)₂), 102.5 (CNH), 113.9 (NCCNH), 120.9 (NCCN), 125.4 (Ar-C), 126.6 (Ar-C), 129.1 (NCCN), 132.3 (Ar-C), 136.3 (Ar-C), 138.0 (Ar-C), 157.6 (Ar-O), 158.8 (HC=N). EI-MS *m/z* calculated for [M]⁺. C₃₈H₄₈N₈O₆Zr₂: 895.28 found 895.7510. Anal. Calcd for C₃₈H₄₈N₈O₆Zr₂: C 50.98, H 5.40, N 12.52. Found: C 50.96, H 5.38, N 12.50.

Complex 2c: Ligand **L2(H)₂** (0.025 g, 0.106 mmol) and Hf(O^{*t*}Bu)₄ (0.050 g, 0.106 mmol) were reacted in 1:1 stoichiometric ratio and the reaction was carried out in similar manner as described for **1a**. Yield 0.05 g, (88%). Mp: 208 °C. ¹H NMR (500 MHz, CDCl₃): δ = 1.44 (s, C(CH₃)₃, 9H), 1.81–1.83 (t, CH₂(CH₃), 3H), 2.57 (s, (CH₃), 9H), 2.75 (s, (CH₃), 3H), 4.20–4.24 (m, CH₂(CH₃), 2H), 6.82 (s, NH, 1H), 7.18 (s, Ar-H, 1H), 7.48 (s, Ar-H, 1H), 8.27 (s, CH=N, 1H). ¹³C NMR (125 MHz, CDCl₃): δ = 20.3 (CH(CH₃)₃), 25.4 (CH₂(CH₃), 32.4 (CH₃), 33.0 (CH₃), 70.5 (O-CH(CH₃)₃), 76.0 (O-CH₂(CH₃), 103.5 (CNH), 114.6 (NCCNH), 121.6 (NCCN), 125.4 (Ar-C), 126.5 (NCCN), 129.1 (Ar-C), 131.6 (Ar-C), 137.9 (Ar-C), 137.9 (Ar-C), 157.5 (Ar-O), 159.3 (HC=N). EI-MS *m/z* calculated for [M]⁺. C₃₈H₄₈N₂₈O₆Hf₂: 1069.82 found 1069.8386. Anal. Calcd for C₃₈H₄₈N₂₈O₆Hf₂: C 42.66, H 4.52, N 10.47. Found: C 42.64, H 4.50, N 10.44.

Complex 3a: Ligand **L3(H)₂** [2-amino-3-((E)-(3-(*tert*-butyl)-2-hydroxy-5-methylbenzylidene)amino)maleonitrile] (0.049 g, 0.175 mmol) and Ti(O^{*i*}Pr)₄ (0.050 g, 0.175 mmol) were reacted in 1:1 stoichiometric ratio and the reaction was carried out in similar manner as described for **1a**. Yield 0.07 g, (93%). Mp: 180 °C. ¹H NMR (500 MHz, CDCl₃): δ = 1.00–1.01 (d, J = 6 Hz, CH(CH₃)₂, 6H), 1.20–1.21 (d, J = 6 Hz, CH(CH₃)₂, 6H), 1.48 (s, C(CH₃)₃, 9H), 2.37 (s, (CH₃), 3H), 4.14–4.16 (m, CH(CH₃)₂, 1H), 4.58–4.63 (m, CH(CH₃)₂, 1H), 6.23 (s, NH, 1H), 7.15 (s, Ar-H, 1H), 7.37 (s, Ar-H, 1H), 8.63 (s, HC=N, 1H). ¹³C NMR (125 MHz, CDCl₃): δ = 20.9 (Ar-CH₃), 25.9 (CH(CH₃)₂), 26.0 (CH(CH₃)₂), 29.6 (C(CH₃)₃), 35.2 (C(CH₃)₃), 68.2 (O-CH(CH₃)₂), 81.5 (O-CH(CH₃)₂), 103.9 (CNH), 113.3 (NCCNH), 122.2 (NCCN), 125.4 (Ar-C), 129.1 (NCCN), 131.1 (Ar-C), 134.2 (Ar-C), 135.6 (Ar-C), 138.0 (Ar-C), 155.9 (Ar-O), 163.6 (HC=N). EI-MS *m/z* calculated for

[M+H]⁺. C₄₄H₆₀N₈O₆Ti₂: 893.73 found 893.6053. Anal. Calcd for C₄₄H₆₀N₈O₆Ti₂: C 59.20, H 6.77, N 12.55. Found: C 59.18, H 6.75, N 12.54.

Complex 3b: Ligand **L3(H)₂** (0.036 g, 0.129 mmol) and Zr(O^{*i*}Pr)₄·PrOH (0.050 g, 0.129 mmol) were reacted in 1:1 stoichiometric ratio and the reaction was carried out in similar manner as described for **1a**. The resulting brown precipitate after solvent evaporation was crystallized from concentrated solution of 1,2-dichloroethane. Yield 0.06 g, (93%). Mp: 186 °C. ¹H NMR (500 MHz, CDCl₃): δ = 0.96–0.97 (d, J = 7.5 Hz, CH(CH₃)₂, 3H), 1.11–1.12 (d, J = 7.5 Hz, CH(CH₃)₂, 3H), 1.27–1.29 (d, J = 7 Hz, CH(CH₃)₂, 6H), 1.65 (s, C(CH₃)₃, 9H), 2.46 (s, (CH₃), 3H), 4.17–4.22 (m, CH(CH₃)₂, 1H), 4.32–4.38 (m, CH(CH₃)₂, 1H), 6.15 (s, NH, 1H), 7.40 (s, Ar-H, 1H), 7.48 (s, Ar-H, 1H), 8.45 (s, HC=N, 1H), [S (1,2-dichloroethane) = 3.74]. ¹³C NMR (125 MHz, CDCl₃): δ = 20.7 (Ar-CH₃), 25.6 (CH(CH₃)₂), 25.9 (CH(CH₃)₂), 26.9 (CH(CH₃)₂), 29.9 (C(CH₃)₃), 35.2 (C(CH₃)₃), 72.9 (O-CH(CH₃)₂), 75.1 (O-CH(CH₃)₂), 102.3 (CNH), 113.8 (NCCNH), 122.3 (NCCN), 125.4 (Ar-C), 128.3 (NCCN), 133.2 (Ar-C), 135.8 (Ar-C), 136.3 (Ar-C), 138.0 (Ar-C), 158.2 (Ar-O), 159.7 (HC=N), [S = 43.5]. EI-MS *m/z* calculated for [M+H]⁺. C₄₄H₆₀N₈O₆Zr₂: 980.44 found 980.1991. Anal. Calcd for C₄₄H₆₀N₈O₆Zr₂: C 53.96, H 6.17, N 11.44. Found: C 53.94, H 6.15, N 11.41.

Complex 3c: Ligand **L3(H)₂** (0.030 g, 0.106 mmol) and Hf(O^{*t*}Bu)₄ (0.050 g, 0.106 mmol) were reacted in 1:1 stoichiometric ratio and the reaction was carried out in similar manner as described for **1a**. Yield 0.05 g, (89%). Mp: 194 °C (decomp). ¹H NMR (500 MHz, CDCl₃): δ = 1.13 (s, C(CH₃)₃, 9H), 1.43–1.45 (t, CH₂(CH₃), 3H), 1.67 (s, C(CH₃)₃, 9H), 2.46 (s, (CH₃), 3H), 4.32–4.36 (m, CH₂(CH₃), 2H), 6.14 (s, NH, 1H), 7.28 (s, Ar-H, 1H), 7.52 (s, Ar-H, 1H), 8.47 (s, CH=N, 1H). ¹³C NMR (125 MHz, CDCl₃): δ = 20.7 (Ar-CH₃), 29.8 (C(CH₃)₃), 31.3 (CH₂(CH₃), 32.0 (C(CH₃)₃), 35.1 (C(CH₃)₃), 67.0 (O-CH₂(CH₃), 72.0 (O-CH(CH₃)₃), 104.1 (CNH), 113.1 (NCCNH), 122.3 (NCCN), 125.4 (Ar-C), 129.2 (NCCN), 133.0 (Ar-C), 136.1 (Ar-C), 138.0 (Ar-C), 138.3 (Ar-C), 155.6 (Ar-O), 159.6 (HC=N). EI-MS *m/z* calculated for [M+H]⁺. C₄₄H₆₀N₈O₆Hf₂: 1154.98 found 1154.2328. Anal. Calcd for C₄₄H₆₀N₈O₆Hf₂: C 45.80, H 5.24, N 9.71. Found: C 45.78, H 5.22, N 9.69.

General procedure for the ROP of ε-CL and rac-LA

A dry reaction vessel of 100 mL capacity kept inside a glove box was equipped with a magnetic bar. A mixture of ε-CL (1 gm, 8.76 mmol) or rac-LA (1 gm, 6.94 mmol) and the desired amount of catalyst were taken in this vessel and then it was closed with a stopper and made air-tight using Teflon tape. The reaction vessel was then taken out side and immersed in an oil bath maintained at 100 °C for ε-CL and 140 °C in case of rac-LA. As the reaction mixture was heated, initially the lactide melted and then became viscous over a period of time ranging from 3 to 21 minutes depending on the catalyst (See Table 1). This indicated the completion of reaction. At this stage the reaction mixture was cooled down to room temperature and dissolved in minimum amount of dichloromethane. The polymer was precipitated by adding excess of cold methanol.

The precipitate was filtered and dried in vacuum to a constant weight. The conversion of ϵ -CL and *rac*-LA were analyzed by ^1H NMR spectroscopic studies of the isolated polymer. Data concerning molecular weights (M_n) and the MWDs (M_w/M_n) of the polymer samples obtained by the ROP of LA were determined by using a GPC instrument with Waters 510 pump and Waters 410 differential refractometer as the detector. The THF columns namely WATERS STRYGEL-HR5, STRYGEL-HR4 and STRYGEL-HR3 each of dimensions (7.8 × 300 mm) were used. Number average molecular weights (M_n) and MWDs (M_w/M_n) of polymers were measured relative to polystyrene standards using THF as solvent at 27 °C.

General procedure for kinetic studies of ϵ -CL and *rac*-LA

The polymerizations of ϵ -CL and *rac*-LA were carried out at $[\text{M}]_0/[\text{Cat}]_0=200:1$ ratio using **3a** at 100 and 140 °C respectively under an argon atmosphere in a sealed tube. Based on the polymerization time for the maximum monomer conversion different time laps of regular intervals were assumed. Then different polymerization reactions were carried out in a sealed tube using 0.5 g of monomer with the required amount of catalyst. In all cases the contents were immersed in a bath at required temperature with constant stirring for the stipulated time as assumed earlier. The each polymer obtained from these polymerization reactions were separately analyzed by ^1H NMR spectroscopy. The $[\text{M}]_{t=0}/[\text{M}]_t$ ratio was calculated by integration of the peak corresponding to the methine protons for the monomer and polymer. The apparent rate constant (k_{app}) values were obtained from the slopes of the best-fit lines.

General procedure for the homopolymerization of epoxides

The epoxides used are *rac*-cyclohexene oxide (CHO), *rac*-propylene oxide (PO) and *rac*-styrene oxide (SO). The procedure of polymerization and method of characterization of the products is very similar to that described for the ROP of *rac*-LA. Here a mixture of *rac*-CHO (1 gm, 10.19 mmol) or *rac*-PO (1 gm, 17.22 mmol) or *rac*-SO (1 gm, 8.32 mmol) with the desired amount of catalyst have been used. However, the reaction temperature and time depended upon the choice of the epoxide (Table 2).

General Procedure for ethylene polymerization

Polymerizations were performed in a 500 ml stainless steel autoclave reactor equipped with a mechanical stirrer and a temperature controller. First 10 μmol of the catalyst was dissolved in 50 ml of toluene along with the required amount of MAO (10 wt % in toluene) was injected into the reactor under argon atmosphere. Once the polymerization temperature (60 °C) was reached, ethylene was purged into the reactor. Then, the reaction mixture was stirred for 30 min under 6.08 bar (6 atm) pressure of ethylene. After 30 min, the polymerization was stopped and subsequently the produced polymer was quenched with acidic methanol (5 mL HCl, 50 mL methanol). The polymer was collected by filtration and dried till under vacuum constant weight was achieved. Molecular weights (M_n and M_w) and the MWDs (M_w/M_n) of polyethylene

samples were determined by GPC instrument with Waters 510 pump and Waters 2414 differential refractometer as the detector. The used column namely WATERS STRYGEL-HR4 of dimensions (4.6 × 300 mm) was connected during the experiment. Measurements were done in 1,2,4-*tri*-chloro benzene (TCB) at 140 °C. Number average molecular weights (M_n) and molecular weight distributions (MWDs) of poly olefins were measured relative to polystyrene standards.

X-ray crystallography

Suitable single crystals of complexes **3a**, **3b** and **3c** were obtained by crystallization from saturated solution of 1,2-dichloroethane or chloroform at room temperature for X-ray structural determinations. Single crystals were mounted on Bruker AXS (Kappa Apex 2) CCD diffractometer equipped with graphite monochromated Mo ($K\alpha$) ($\lambda = 0.7107 \text{ \AA}$) radiation source. The data were collected with 100% completeness for θ up to 25°. ω and ϕ scans was employed to collect the data. The frame width for ω for was fixed to 0.5° for data collection. The frames were subjected to integration and data were reduced for Lorentz and polarization corrections using SAINT-NT. The multi-scan absorption correction was applied to the data set. All structures were solved using SIR-92 and refinement was done using SHELXL-97.¹⁸ Location of all the hydrogen atoms could be found in the difference Fourier map. The hydrogen atoms attached to carbon atoms were fixed at chemically meaningful positions and were allowed to ride with the parent atom during refinement. These data were deposited with CCDC with the numbers: CCDC 1438097–1438099.

Conclusions

In conclusion, dinuclear group 4 complexes of tridentate [NNO]-type of Schiff-base ligands have been synthesized in good yields and completely characterized by NMR and Mass techniques and the solid state structures of Ti, Zr and Hf complexes of a given ligand have been elucidated by single crystal X-ray diffraction studies. All these complexes performed as highly active in ROP of ϵ -CL and *rac*-LA under industrially preferred melt conditions. The narrow PDI values of PCL and PLA suggested the occurrences of living polymerization. All complexes acted as stereoselective initiators, as the PLA obtained from *rac*-LA featured good degree of heterotacticity. Mechanistic studies performed in the ROP of *rac*-LA suggested the coordination-insertion mechanism. Kinetic studies revealed the first order rate constant with respect to ϵ -CL and *rac*-LA conversions. All complexes showed moderate activity for ROP of *rac*-epoxides, such as, CHO, PO and SO. Finally, application of these complexes directed towards ethylene polymerization, where these complexes exhibited good catalytic activity for producing PE upon activation with MAO. Particularly the complexes, bearing bulky *tert*-butyl *ortho*-phenolate substituent, exhibited high catalytic activity.

Acknowledgements

This work was supported by the Department of Science and Technology, New Delhi. We thank IIT Madras for financial support. Instrumentation facilities were availed from Department of Chemistry and SAIF, IIT Madras.

Notes and references

- (a) T. M. Ovitt and G. W. Coates, *J. Am. Chem. Soc.*, 2002, **124**, 1316–1326. (b) D. J. Darensbourg and O. Karroonnirun, *Macromolecules*, 2010, **43**, 8880–8886. (c) S. Sun, K. Nie, Y. Tan, B. Zhao, Y. Zhang, Q. Shen and Y. Yao, *Dalton Trans.*, 2013, **42**, 2870–2878. (d) M. Hayatifar, F. Marchetti, G. Pampaloni and S. Zacchini, *Inorg. Chem.*, 2013, **52**, 4017–4025. (e) W. Yi and H. Ma, *Inorg. Chem.*, 2013, **52**, 11821–11835. (f) M. O. Miranda, Y. DePorre, H. Vazquez-Lima, M. A. Johnson, D. J. Marell, C. J. Cramer and W. B. Tolman, *Inorg. Chem.*, 2013, **52**, 13692–13701. (g) S. Yang, K. Nie, Y. Zhang, M. Xue, Y. Yao and Q. Shen, *Inorg. Chem.*, 2014, **53**, 105–115. (h) Y. L. Hsieh, Y. C. Lin, G. H. Lee and C. H. Peng, *Polymer*, 2015, **56**, 237–244.
- (a) A. C. Albertsson and I. K. Varma, *Biomacromolecules*, 2003, **4**, 1466–1486. (b) C. S. Ha and J. A. Gardella, *Chem. Rev.*, 2005, **105**, 4205–4232.
- (a) S. Gendler, S. Segal, I. Goldberg, Z. Goldschmidt and M. Kol, *Inorg. Chem.*, 2006, **45**, 4783–4790. (b) A. J. Chmura, M. G. Davidson, M. D. Jones, M. D. Lunn, M. F. Mahon, A. F. Johnson, P. Khunkamchoo, S. L. Roberts and S. S. F. Wong, *Macromolecules*, 2006, **39**, 7250–7257. (c) C. M. Manna, M. Shavit and E. Y. Tshuva, *J. Organomet. Chem.*, 2008, **693**, 3947–3950. (d) A. J. Chmura, D. M. Cousins, M. G. Davidson, M. D. Jones, M. D. Lunn and M. F. Mahon, *Dalton Trans.*, 2008, 1437–1443. (e) A. J. Chmura, M. G. Davidson, C. J. Frankis, M. D. Jones and M. D. Lunn, *Chem. Commun.*, 2008, 1293–1295. (f) A. L. Zelikoff, J. Kopilov, I. Goldberg, G. W. Coates and M. Kol, *Chem. Commun.*, 2009, 6804–6806. (g) A. D. Schwarz, A. L. Thompson, and P. Mountford, *Inorg. Chem.*, 2009, **48**, 10442–10454. (h) M. Hu, M. Wang, H. Zhu, L. Zhang, H. Zhang and L. Sun, *Dalton Trans.*, 2010, **39**, 4440–4446. (i) F. Zhang, H. Song and G. Zi, *J. Organomet. Chem.*, 2010, **695**, 1993–1999. (j) E. Sergeeva, J. Kopilov, I. Goldberg and M. Kol, *Inorg. Chem.*, 2010, **49**, 3977–3979. (k) L. C. Liang, Y. L. Hsu and S. T. Lin, *Inorg. Chem.*, 2011, **50**, 3363–3372. (l) S. L. Hancock, M. F. Mahon, G. K. Köhn and M. D. Jones, *Eur. J. Inorg. Chem.*, 2011, 4596–4602. (m) S. L. Hancock, M. F. Mahon and M. D. Jones, *Dalton Trans.*, 2011, **40**, 2033–2037. (n) A. Stopper, I. Goldberg and M. Kol, *Inorg. Chem. Commun.*, 2011, **14**, 715–718. (o) J. C. Buffet, A. N. Martin, M. Kol and J. Okuda, *Polym. Chem.*, 2011, **2**, 2378–2384. (p) A. Stopper, J. Okuda and M. Kol, *Macromolecules*, 2012, **45**, 698–704. (q) L. G. Alves, F. Hild, R. F. Munhá, L. F. Veiros, S. Dagonne and A. M. Martins, *Dalton Trans.*, 2012, **41**, 14288–14298. (r) A. Sauer, J. C. Buffet, T. P. Spaniol, H. Nagae, K. Mashima and J. Okuda, *Inorg. Chem.*, 2012, **51**, 5764–5770. (s) L. Azor, C. Bailly, L. Brelot, M. Henry, P. Mobian and S. Dagonne, *Inorg. Chem.*, 2012, **51**, 10876–10883. (t) A. Sauer, A. Kapelski, C. Fliedel, S. Dagonne, M. Kol and J. Okuda, *Dalton Trans.*, 2013, **42**, 9007–9023. (u) R. R. Gowda and E. Y. X. Chen, *Dalton Trans.*, 2013, **42**, 9263–9273. (v) L. C. Liang, S. T. Lin, C. C. Chien and M. T. Chen, *Dalton Trans.*, 2013, **42**, 9286–9293. (w) C. Y. Li, C. J. Yu and B. T. Ko, *Organometallics*, 2013, **32**, 172–180. (x) R. L. Webster, N. Noroozi, S. G. Hatzikiriakos, J. A. Thomson and L. L. Schafer, *Chem. Commun.*, 2013, **49**, 57–59. (y) C. J. Chuck, M. G. Davidson, G. G. Sart, P. K. I. Mitseva, G. I. K. Köhn and L. B. Manton, *Inorg. Chem.*, 2013, **52**, 10804–10811.
- (a) M. J. Go, J. M. Lee, K. M. Lee, C. H. Oh, K. H. Park, S. H. Kim, M. Kim, H. R. Park, M. H. Park, Y. Kim and A. Lee, *Polyhedron*, 2014, **67**, 286–294. (b) M. Sietzen, H. Wadehoff and J. Ballmann, *Organometallics*, 2014, **33**, 612–615. (c) Q. Sun, Y. Wang, D. Yuan, Y. Yao and Q. Shen, *Organometallics*, 2014, **33**, 994–1001. (d) R. R. Gowda, L. Caporaso, L. Cavallo and E. Y. X. Chen, *Organometallics*, 2014, **33**, 4118–4130. (e) F. D. Monica, E. Luciano, G. Roviello, A. Grassi, S. Milione and C. Capacchione, *Macromolecules*, 2014, **47**, 2830–2841. (f) N. Zhao, G. Hou, X. Deng, G. Zi and M. D. Walter, *Dalton Trans.*, 2014, **43**, 8261–8272.
- (a) R. R. Gowda, D. Chakraborty and V. Ramkumar, *Eur. J. Inorg. Chem.*, 2009, 2981–2993. (b) T. K. Saha, B. Rajashekhar, R. R. Gowda, V. Ramkumar and D. Chakraborty, *Dalton Trans.*, 2010, **39**, 5091–5093. (c) R. R. Gowda, D. Chakraborty and V. Ramkumar, *Polymer*, 2010, **51**, 4750–4759. (d) R. R. Gowda, D. Chakraborty and V. Ramkumar, *J. Organomet. Chem.*, 2011, **696**, 572–580. (e) Saha, T. K.; Ramkumar, V.; Chakraborty, D. *Inorg. Chem.* 2011, **50**, 2720–2722. (f) R. R. Gowda, D. Chakraborty and V. Ramkumar, *Inorg. Chem. Commun.*, 2011, **14**, 1777–1782. (g) T. K. Saha, B. Rajashekhar, D. Chakraborty, *RSC Advances*, 2012, **2**, 307–318. (h) T.K. Saha, M. Mandal, V. Ramkumar and D. Chakraborty, *New J. Chem.*, 2013, **37**, 949–960. (i) S. Pappuru, E. R. Chokkapu, D. Chakraborty and V. Ramkumar, *Dalton Trans.*, 2013, **42**, 16412–16427. (j) D. Chakraborty, D. Mandal, V. Ramkumar, D. Subramanian and J. V. Sundar, *Polymer*, 2015, **56**, 157–170. (k) M. Mandal, D. Chakraborty and V. Ramkumar, *RSC Advances*, 2015, **5**, 28536–28553. (l) S. K. Roymuhury, D. Chakraborty and V. Ramkumar, *Dalton Trans.*, 2015, **44**, 10352–10367. (m) S. K. Roymuhury, D. Chakraborty and V. Ramkumar, *New J. Chem.*, 2015, **39**, 5218–5230. (n) B. Rajashekhar, S. K. Roymuhury, D. Chakraborty and V. Ramkumar, *Dalton Trans.*, 2015, **44**, 16280–16293.
- (a) H. Rembold, Arlesheim, D. Baumann, Birsfelden and J. Habermeier, *U.S. Patent* 1973, **3,779,988**. (b) A. J. Ullree, *Encyclopedia of Polymer Science and Engineering*; John Wiley and Sons: New York, 1986, **6**, 733–755. (c) J. E. Bolick, A. W. Jensen, *Encyclopedia of Chemical Technology*, 4th ed.; Kirk-Othmer, Ed.; John Wiley and Sons: New York, 1993, **10**, 624–638.
- (a) R. Bacskai, *J. Polym. Sci., Part A: Polym. Chem.*, 1963, **1**, 2777–2790. (b) Y. Fukuchi, T. Takahashi, H. Noguchi, M. Saburi and Y. Uchida, *J. Polym. Sci., Part C: Polym. Lett.*, 1988, **26**, 401–403. (c) N. Suzuki, M. Miyama, T. Takahashi, H. Noguchi, M. Saburi and Y. Uchida, *J. Polym. Sci., Part A: Polym. Chem.*, 1992, **30**, 2067–2069. (d) M. Thiam and N. Spassky, *Macromol. Chem. Phys.*, 1999, **200**, 2107–2110. (e) T. Sârbu and E. J. Beckman, *Macromolecules*, 1999, **32**, 6904–6912. (f) L. Ge, Q. Huang, Y. Zhang and Z. Shen, *Eur. Polym. J.*, 2000, **36**, 2699–2705. (g) K. L. Peretti, H. Ajiro, C. T. Cohen, E. B. Lobkovsky and G. W. Coates, *J. Am. Chem. Soc.*, 2005, **127**, 11566–11567. (h) W. Hirahata, R. M. Thomas, E. B. Lobkovsky and G. W. Coates, *J. Am. Chem. Soc.*, 2008, **130**, 17658–17659. (i) H. Ajiro, K. L. Peretti, E. B. Lobkovsky and G. W. Coates, *Dalton Trans.*, 2009, 8828–8830. (j) R. M. Thomas, P. C. B. Widger, S. M. Ahmed, R. C. Jeske, W. Hirahata, E. B. Lobkovsky and G. W. Coates, *J. Am. Chem. Soc.*, 2010, **132**, 16520–16525. (k) S. M. Ahmed, A. Poater, M. I. Childers, P. C. B. Widger, A. M. LaPointe, E. B. Lobkovsky, G. W. Coates and L. Cavallo, *J. Am. Chem. Soc.*, 2013, **135**, 18901–18911. (l) N. D. Harrold, Y. Li and M. H. Chisholm, *Macromolecules*, 2013, **46**, 692–698. (m) H. Plommer, I. Reim and F. M. Kerton, *Dalton Trans.*, 2015, **44**, 12098–12102.
- (a) S. Matsui, M. Mitani, J. Saito, Y. Tohi, H. Makio, N. Matsukawa, Y. Takagi, K. Tsuru, M. Nitabaru, T. Nakano, H.

- Tanaka, N. Kashiwa and T. Fujita, *J. Am. Chem. Soc.*, 2001, **123**, 6847–6856. (b) S. Ishii, J. Saito, M. Mitani, J. Mohri, N. Matsukawa, Y. Tohi, S. Matsui, N. Kashiwa and T. Fujita, *J. Mol. Catal. A: Chem.*, 2002, **179**, 11–16. (c) S. Segal, I. Goldberg and M. Kol, *Organometallics*, 2005, **24**, 200–202. (d) S. Zhang and K. Nomura, *J. Am. Chem. Soc.*, 2010, **132**, 4960–4965. (e) H. Makio, H. Terao, A. Iwashita and T. Fujita, *Chem. Rev.*, 2011, **111**, 2363–2449. (f) H. Gao, H. Hu, F. Zhu and Q. Wu, *Chem. Commun.*, 2012, **48**, 3312–3314. (g) J. Lai, W. Zhao, W. Yang, C. Redshaw, T. Liang, Y. Liuc and W. H. Sun, *Polym. Chem.*, 2012, **3**, 787–793. (h) D. Shoken, M. Sharma, M. Botoshansky, M. Tamm and M. S. Eisen, *J. Am. Chem. Soc.*, 2013, **135**, 12592–12595.
- 9 (a) M. Mitani, T. Nakano and T. Fujita, *Chem. Eur. J.*, 2003, **9**, 2396–2403. (b) K. Michiue and R. F. Jordan, *Organometallics*, 2004, **23**, 460–470. (c) N. R. S. Basso, P. P. Greco, C. L. P. Carone, P. R. Livotto, L. M. T. Simpl'icio, Z. N. Rocha, G. B. Galland and J. H. Z. Santos, *J. Mol. Catal. A: Chem.*, 2007, **267**, 129–136. (d) G. H. Zohuri, S. Damavandi, R. Sandaroods, and S. Ahmadjo, *Polym. Bull.*, 2011, **66**, 1051–1062. (e) P. Hu, J. Q. Wang, F. Wang and G. X. Jin, *Chem. Eur. J.*, 2011, **17**, 8576–8583. (f) H. Hamaki, N. Takeda, M. Nabika and N. Tokitoh, *Macromolecules*, 2012, **45**, 1758–1769. (g) X. C. Shi and G. X. Jin, *Organometallics*, 2012, **31**, 7198–7205. (h) I. E. Nifant'ev, P. V. Ivchenko, V. V. Bagrov, S. M. Nagy, S. Mihan, L. N. Winslow and A. V. Churakov, *Organometallics*, 2013, **32**, 2685–2692. (i) K. Huang, S. Zhou, D. Zhang, X. Gao, Q. Wang and Y. Lin, *J. Organomet. Chem.*, 2013, **741–742**, 83–90. (j) R. Zhao, T. Liu, L. Wang and H. Ma, *Dalton Trans.*, 2014, **43**, 12663–12677. (k) N. V. Kulkarni, T. Elkin, B. Tumaniskii, M. Botoshansky, L. J. W. Shimon and M. S. Eisen, *Organometallics*, 2014, **33**, 3119–3136.
- 10 (a) H. Makio, N. Kashiwa and T. Fujita, *Adv. Synth. Catal.*, 2002, **344**, 477–493. (b) M. Mitani, J. Saito, S. Ishii, Y. Nakayama, H. Makio, N. Matsukawa, S. Matsui, J. Mohri, R. Furuyama, H. Terao, H. Bando, H. Tanaka and T. Fujita, *Chem. Rec.*, 2004, **4**, 137–158. (c) Y. Nakayama, J. Saito, H. Bando and T. Fujita, *Chem. Eur. J.*, 2006, **12**, 7546–7556. (d) S. Kinoshita, K. Kawamura and T. Fujita, *Chem. Asian J.*, 2011, **6**, 284–290.
- 11 M. J. MacLachlan, M. K. Park and L. K. Thompson, *Inorg. Chem.*, 1996, **35**, 5492–5499.
- 12 (a) K. A. M. Thakur, R. T. Kean, E. S. Hall, J. J. Kolstad, T. A. Lindgren, M. A. Doscotch, J. I. Siepmann and E. J. Munson, *Macromolecules*, 1997, **30**, 2422–2428. (b) B. M. Chamberlain, M. Cheng, D. R. Moore, T. M. Ovitt, E. B. Lobkovsky and G. W. Coates, *J. Am. Chem. Soc.*, 2001, **123**, 3229–3238. (c) T. M. Ovitt and G. W. Coates, *J. Am. Chem. Soc.*, 2002, **124**, 1316–1326. (d) M. T. Zell, B. E. Padden, A. J. Paterick, K. A. M. Thakur, R. T. Kean, M. A. Hillmyer and E. J. Munson, *Macromolecules*, 2002, **35**, 7700–7707.
- 13 (a) G. J. P. Britovsek, M. Bruce, V. C. Gibson, B. S. Kimberley, P. J. Maddox, S. Mastroianni, S. J. McTavish, C. Redshaw, G. A. Solan, S. Strömberg, A. J. P. White and D. J. Williams, *J. Am. Chem. Soc.*, 1999, **121**, 8728–8740. (b) J. G. P. Britovsek, S. Mastroianni, G. A. Solan, S. P. D. Baugh, C. Redshaw, V. C. Gibson, A. J. P. White, D. J. Williams and M. R. J. Elsegood, *Chem. Eur. J.*, 2000, **6**, 2221–2231.
- 14 S. Koltzenburg, *J. Mol. Catal. A: Chem.*, 1997, **116**, 355–363.
- 15 F. Gornshstein, M. Kapon, M. Botoshansky and M. S. Eisen, *Organometallics*, 2007, **26**, 497–507.
- 16 V. Volkis, E. Smolensky, A. Lisovskii and M. S. Eisen, *J. Polym. Sci., Part A: Polym. Chem.*, 2005, **43**, 4505–4516.
- 17 G. F. Moore, J. D. Megiatto Jr, M. Hamburger, M. Gervaldo, G. Kodis, T. A. Moore, D. Gust and A. L. Moore, *Photochem. Photobiol. Sci.*, 2012, **11**, 1018–1025.
- 18 G. M. Sheldrick, SHELXL97. Program for crystal structure refinement, Göttingen, Germany.

View Article Online
DOI: 10.1039/C5RA26721H

Graphical abstract

A series of new dinuclear group 4 complexes containing [NNO]-type ligands are utilized as catalysts for polymerization reactions.

